Fraunhofer
IISB

Fraunhofer Institute for Integrated
Systems and Device Technology IISB

Simulation for Reliability and Testing

Sebastian A. Letz
IISB Annual Symposium 2023
October 12, 2023, Fraunhofer IISB, Erlangen, Germany

Contents

1. Introduction to Simulation for Reliability and Testing
2. Materials Modeling for Sintered Silver
   - Representative-Volume-Element Analysis
   - Scale Transition Modeling
   - A Plastic Yield Locus Model
3. Adhesion Strength of Metallic Thin Films
   - Cross-Sectional-Nanoindentation (CSN)
   - CSN Analysis by FEM Modeling
4. Conclusions

Introduction to Simulation for Reliability and Testing

Simulation Across the Lifetime and Reliability Estimation Chain

Electric Simulation

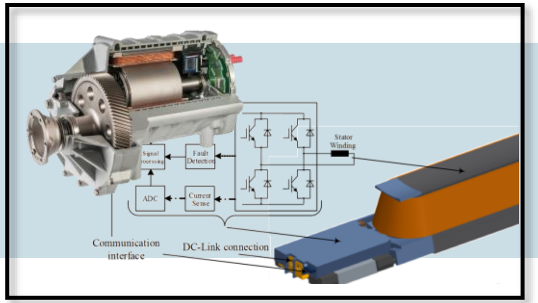

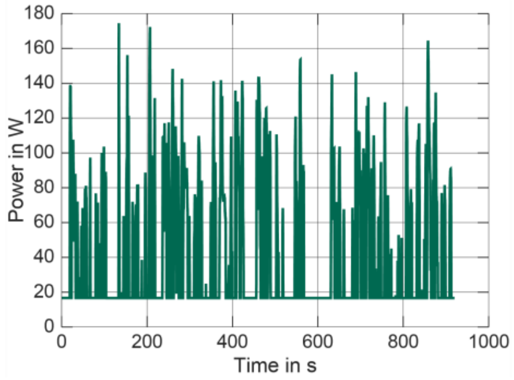

Experimental Validation / Calibration

Thermal Simulation

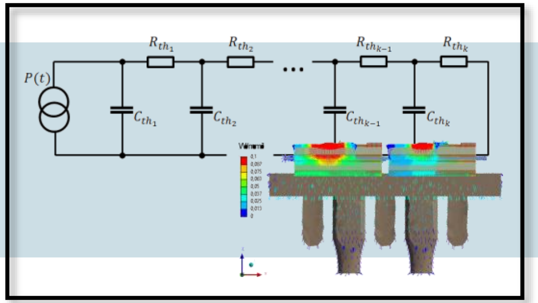

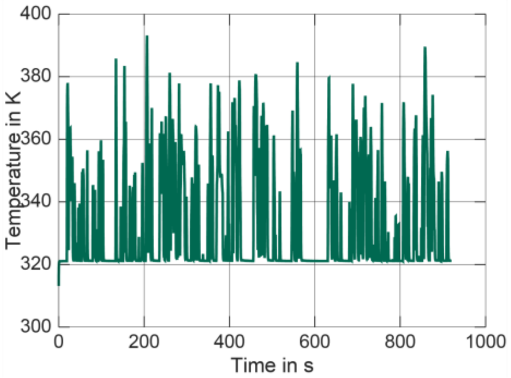

Experimental Validation / Calibration

Structural Simulation

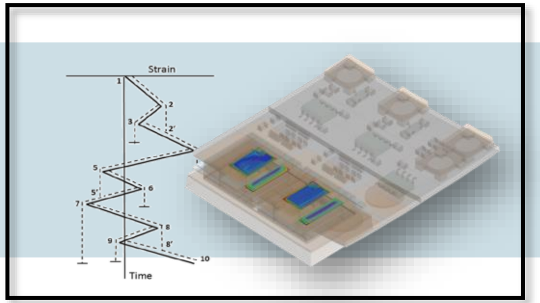

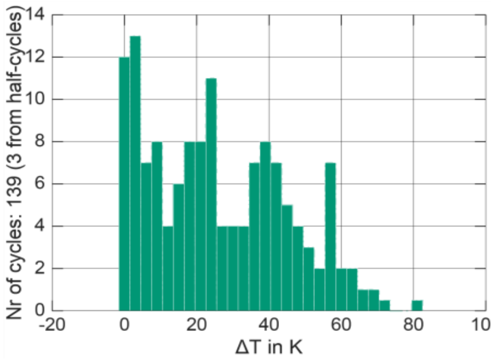

Experimental Validation / Calibration

Lifetime Prognosis

$$D = \sum_{i=1}^{k} n_i \cdot \left[A \cdot \Delta T_{j,i}^{-\alpha} \cdot e^{\frac{E_A}{k_B T_{jm,i}}} \cdot \frac{C + t_{on,i}^{-\gamma}}{C + 2^{-\gamma}} \right]^{-1}$$

$$f(t) = \frac{dF(t)}{dt} = \frac{\beta}{\alpha} \left(\frac{t}{\alpha}\right)^{\beta-1} e^{-\left(\frac{t}{\alpha}\right)^{\beta}}$$

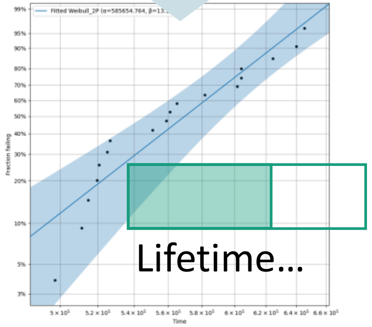

Experimental Validation / Calibration

Introduction to Simulation for Reliability and Testing

Some Failure Mechanisms

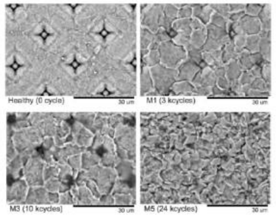

Ali Ibrahim, Zoubir Khatir, Jean-Pierre Ousten, Richard Lallemand, Stefan V. Mollov, etal.. Using of Bond-Wire Resistance as Ageing Indicator of Semiconductor Power Modules. Microelectronics Reliability, Elsevier, 2020, MicroelectronicsReliability, 114, 10.1016/j.microrel.2020.113757.

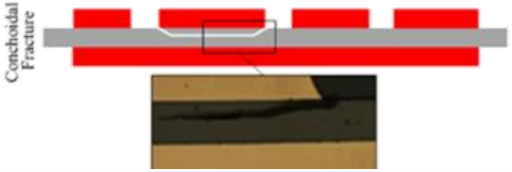

A. J. George, M. Breitenbach, J. Zipprich, M. Klingler and M. Nowottnick, "Nonconchoidal Fracture in Power Electronics Substrates due to Delamination in Baseplate Solder Joints," 2018 7th Electronic System-Integration Technology Conference (ESTC), 2018, pp. 1-6, doi: 10.1109/ESTC.2018.8546472.

*S. Yang, D. Xiang, A. Bryant, P. Mawby, L. Ran and P. Tavner, "Condition Monitoring for Device Reliability in Power Electronic Converters: A Review," in *IEEE Transactions on Power Electronics*, vol. 25, no. 11, pp. 2734-2752, Nov. 2010, doi: 10.1109/TPEL.2010.2049377.

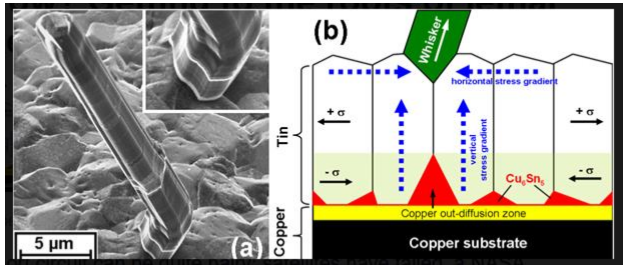

M. Sobiech, M. Wohlschlögel, U. Welzel, E. J. Mittemeijer, W. Hügel, A. Seekamp, W. Liu, and G. E. Ice, "Local, submicron, strain gradients as the cause of Sn whisker growth", Appl. Phys. Lett. 94, 221901 (2009) https://doi.org/10.1063/1.3147864

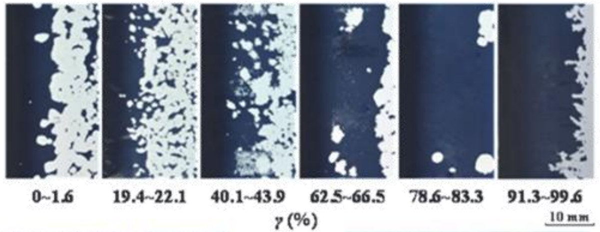

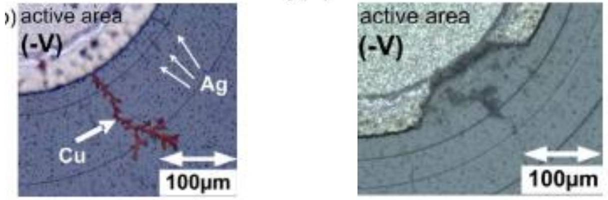

C. Zorn and N. Kaminski, "Acceleration of temperature humidity bias (THB) testing on IGBT modules by high bias levels," 2015 IEEE 27th International Symposium on Power Semiconductor Devices & IC's (ISPSD), 2015, pp. 385-388, doi: 10.1109/ISPSD.2015.7123470.

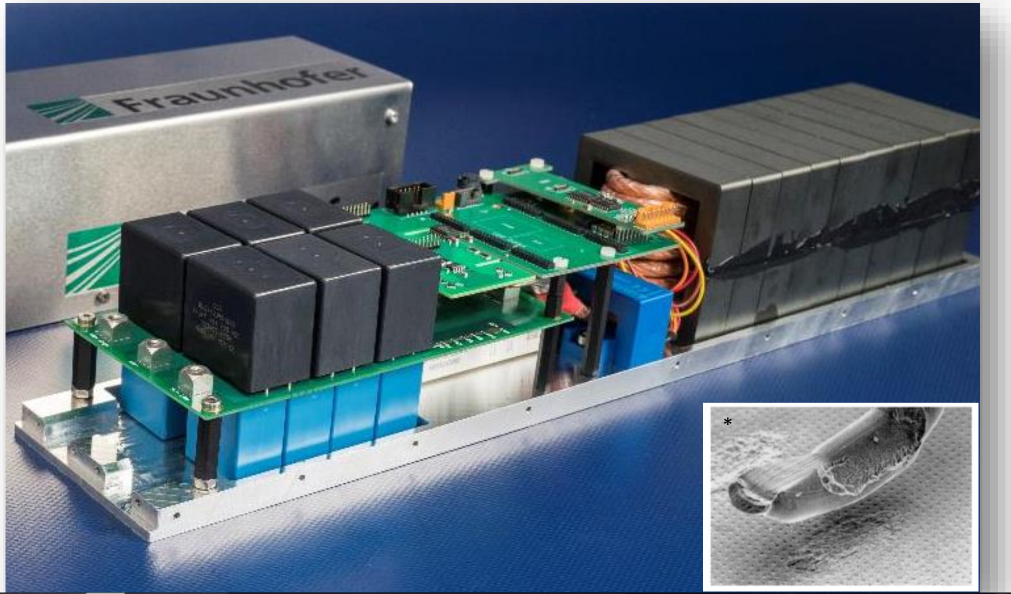

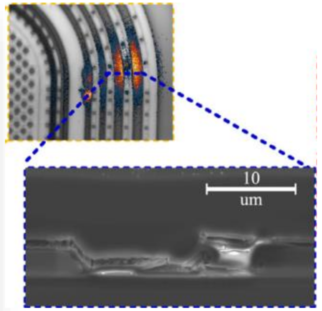

J. Leppänen, J. Ingman, J.-H. Peters, M. Hanf, R. Ross, G. Koopmans, J. Jormanainen, A. Forsström, G. Ross, N. Kaminski, V. Vuorinen, Aluminium corrosion in power semiconductor devices, Microelectronics Reliability, Volume 137, 2022, 114766, ISSN 0026-2714, https://doi.org/10.1016/j.microrel.2022.114766.

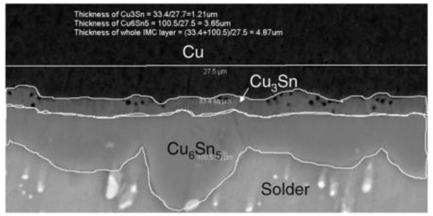

Weiqun Peng, Eduardo Monlevade, Marco E. Marques, Effect of thermal aging on the interfacial structure of SnAgCu solder joints on Cu, Microelectronics Reliability, Volume 47, Issue 12, 2007, Pages 2161-2168, ISSN 0026-2714, https://doi.org/10.1016/j.microrel.2006.12.006.

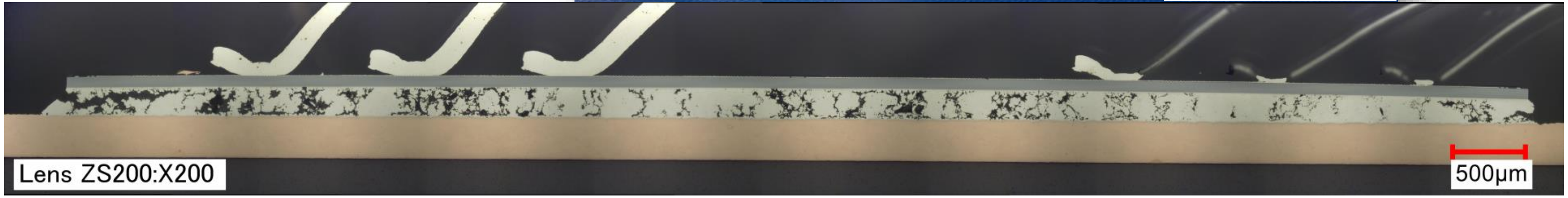

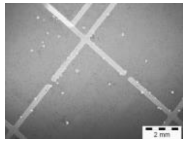

W. Grimm, "Ageing of Film Capacitors", ECPE Workshop, Lifetime Modelling and Simulation, 3 – 4 July 2013, Dusseldorf, Germany

J. Flicker, R. Kaplar, M. Marinella and J. Granata, "Lifetime testing of metallized thin film capacitors for inverter applications," 2013 IEEE 39th Photovoltaic Specialists Conference (PVSC), Tampa, FL, USA, 2013, pp. 3340-3342, doi: 10.1109/PVSC.2013.6745166.

Introduction to Simulation for Reliability and Testing

FEM-based Lifetime Estimation

- FEM-based load analysis and robustness estimation:
  → Inter-/Extrapolation for geometry and materials
- Plastic strain energy density range during thermal cycle feeds damage model for low cycle fatigue failure

$$\mathit{Plastic\ Dissipation\ Power} = \boldsymbol{\sigma} : \dot{\boldsymbol{\varepsilon}}^{p}$$

$$W_p = \frac{1}{V} \int_V \int_t (\boldsymbol{\sigma} : \dot{\boldsymbol{\varepsilon}}^{p})\, dt\, dV$$

- Material Model: Relation between stress and strain (inelasticity) must be well known and calibrated
- Damage Model: Relation between failure and stressor must be calibrated (fatigue, creep, etc.)

FEM Simulation Model

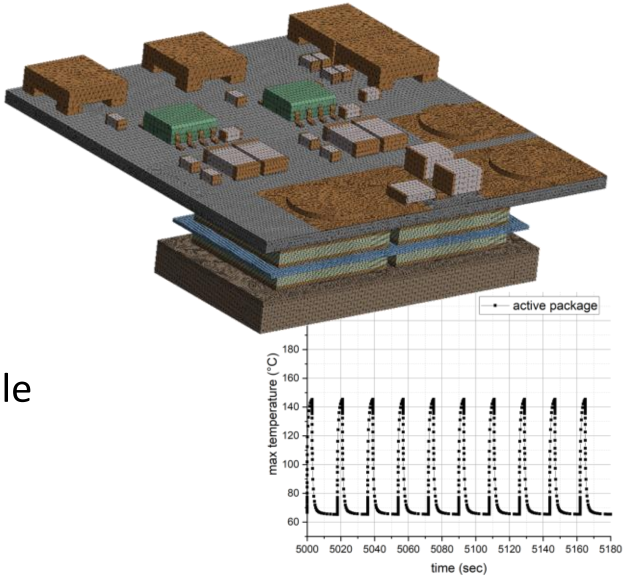

FEA

Plastic Strain Energy Density W_{in} in Sinter Layer

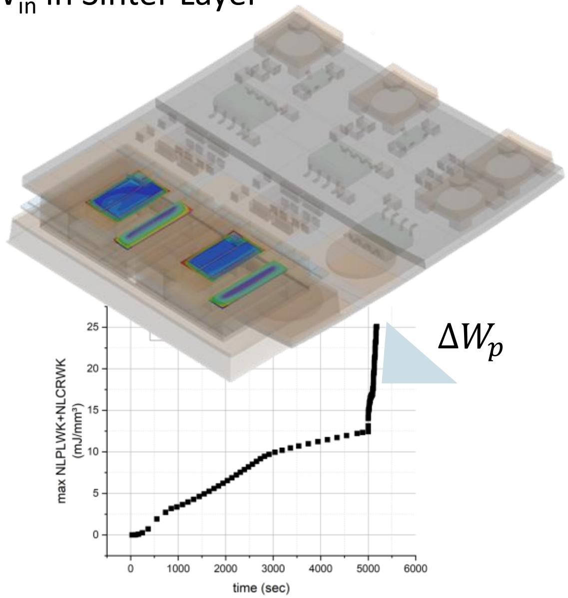

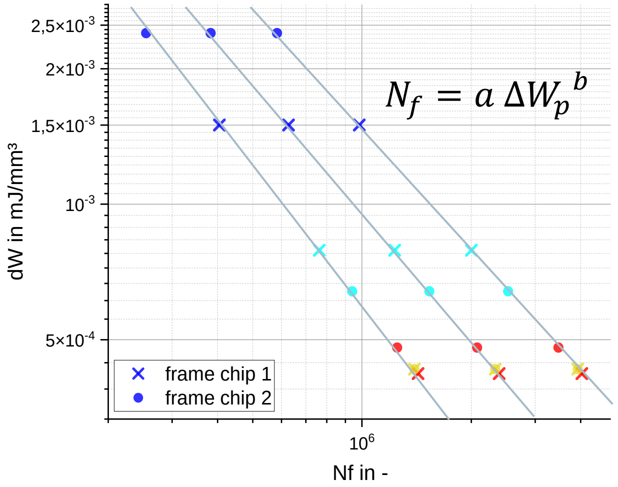

Damage Model: Coffin-Manson Type obtained by Power Cycling Experiments

Materials Modeling for Sintered Silver

Problem Description

- Sintered silver used as interconnection material
- Thin interconnection layer (10-50 µm) is porous
- Strong influence of porosity on material behavior
- Pure experimental investigations are inefficient
- Combined experimental-numerical investigation

- Following slides are based on:

S.A. Letz, D. Zhao, M. März, Mesostructural impact on the macroscopic stress state and yield locus of porous polycrystalline silver, Materials & Design, Volume 219, 2022, 110785, ISSN 0264-1275, https://doi.org/10.1016/j.matdes.2022.110785.

Power module with sintered silver chip interconnects

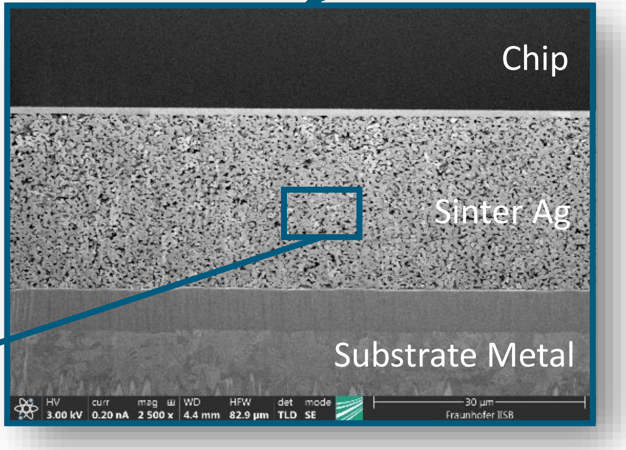

FIB cross-section of sintered silver interconnect layer

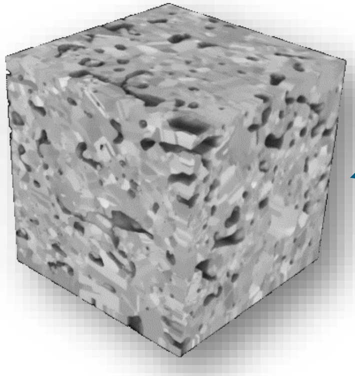

Reconstructed volume element of sintered silver interconnect layer showing significant amount of porosity

Materials Modeling for Sintered Silver

Representative-Volume-Element Analysis

- FIB tomography for different sintering states
- Evaluate sinter structure properties and their trajectories
- Construct triangular surface models of porosity data
- Invert surface models and fill to obtain volume models
- Discretization / Finite-Element Meshing in FEM software

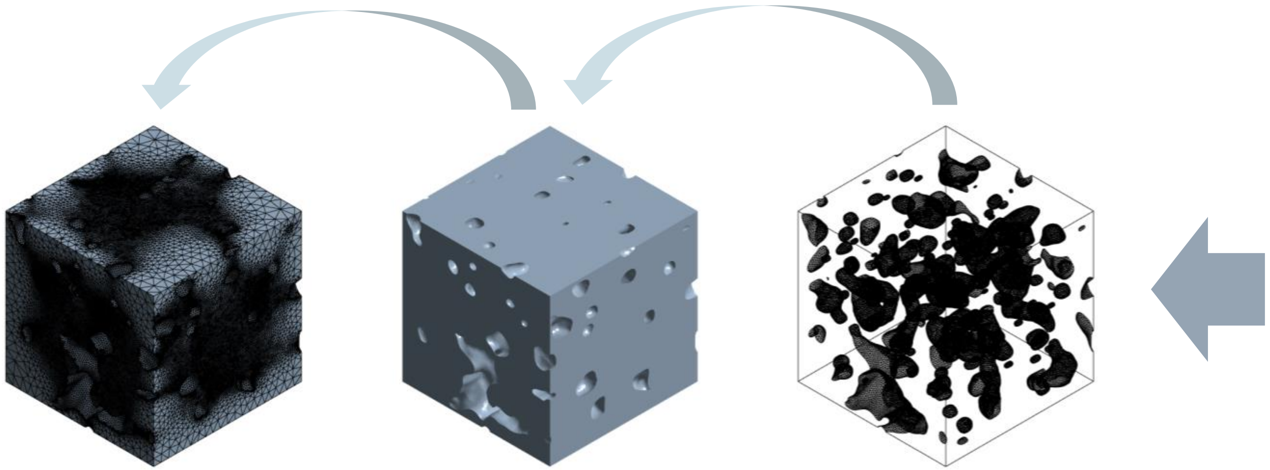

Meshed Volume Model

Volume Model

Inverted Surface Model

FIB Tomography

Porosity Model Reconstruction

Pore Structure Analysis

FEA Model Reconstruction

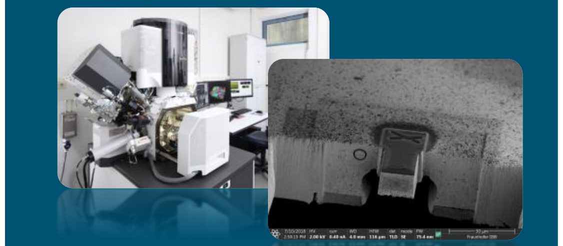

Automated FIB Tomography

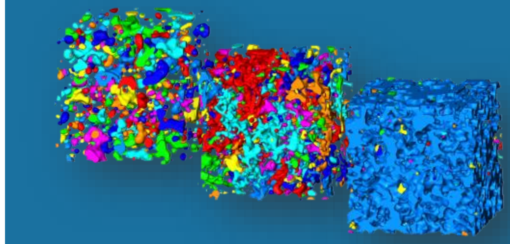

Porosity Surface Models

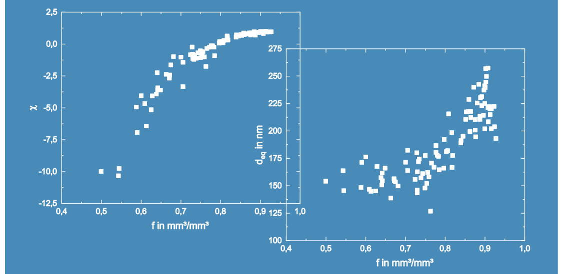

Pore Structure Properties

Materials Modeling for Sintered Silver

Representative-Volume-Element Analysis

- Mechanical FEA to study influence of sintered structure on macroscopic stress state and plastic yield locus
- Size study (1-5 µm edge length) to identify representative volume element (RVE) → 3 µm edge length for RVE
- Define control node per face and couple normal DOFs
- Parametric boundary conditions applied to control nodes

$$\bar{u}_1^{top} = \bar{\varepsilon}\, LRV_E(\beta + \alpha)$$

$$\bar{u}_2^{top} = \bar{\varepsilon}\, LRV_E(\beta - \alpha)$$

$$\bar{u}_3^{top} = \bar{\varepsilon}\, LRV_E\, \beta$$

$$\bar{u}_1^{bot} = \bar{u}_2^{bot} = \bar{u}_3^{bot} = 0$$

- Homogenization by measuring forces at control nodes
- Elastic – perfect plastic matrix material behavior

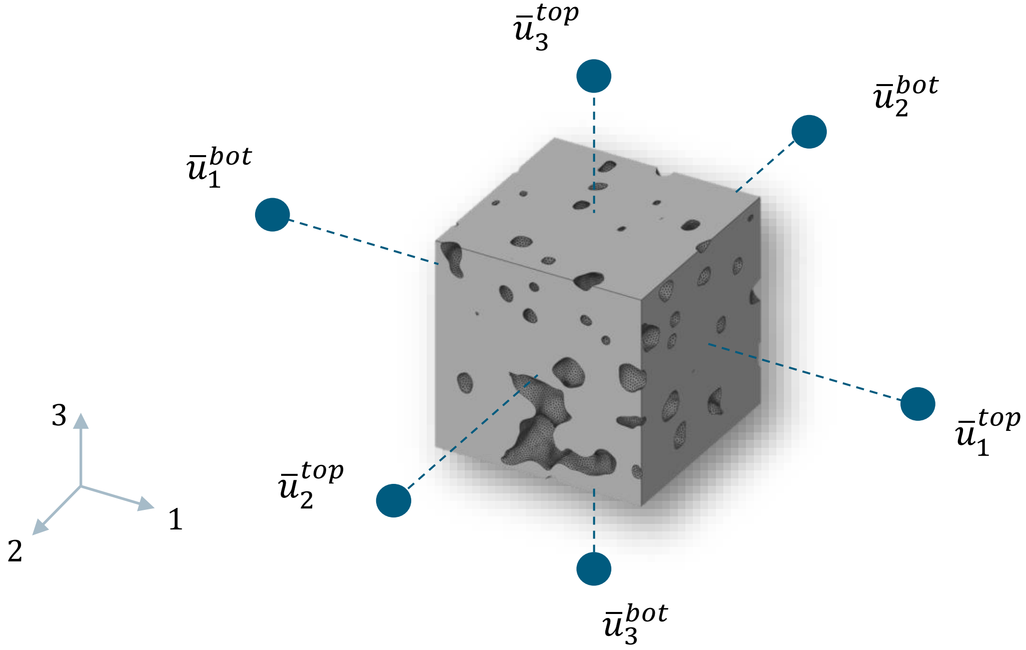

Computational Homogenization Approach

Materials Modeling for Sintered Silver

Scale Transition Modeling

- Macroscopic stress state as function of applied stress state (shear and hydrostatic) and sintered structure
- Formulation of new scale transition model
- Pore structure properties can be homogenized
- Continuity tensor is composed of impact functions

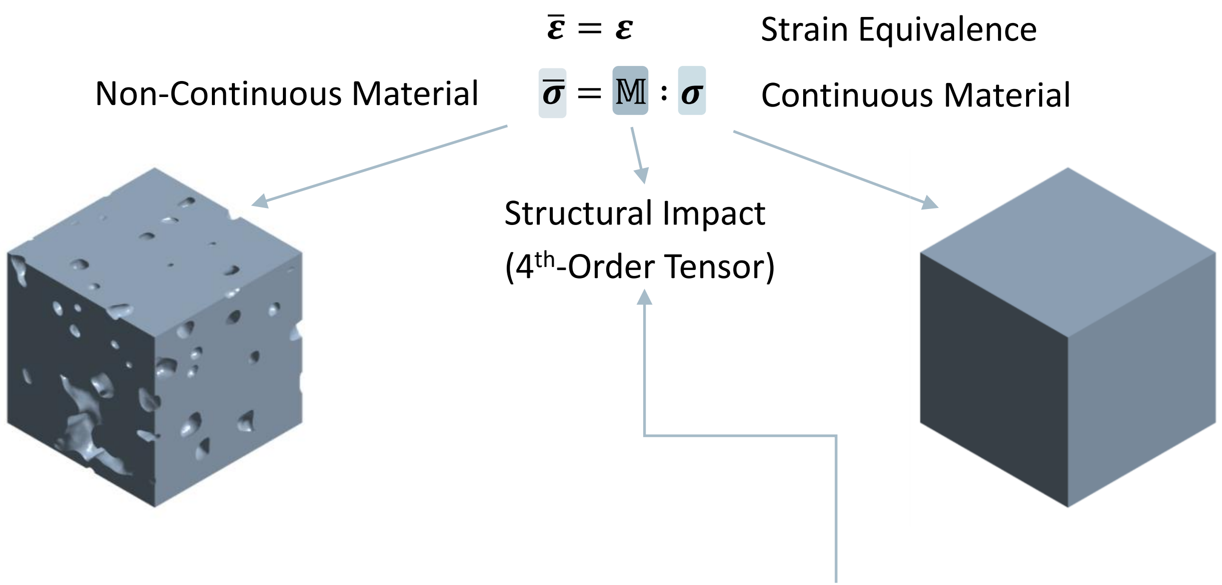

$\bar{\boldsymbol{\varepsilon}} = \boldsymbol{\varepsilon}$ Strain Equivalence

Non-Continuous Material $\bar{\boldsymbol{\sigma}} = \mathbb{M} : \boldsymbol{\sigma}$ Continuous Material

Structural Impact
(4^{th}-Order Tensor)

Pore Structure Properties

$$d_{eq}, SF, N, \chi, f, S_m$$

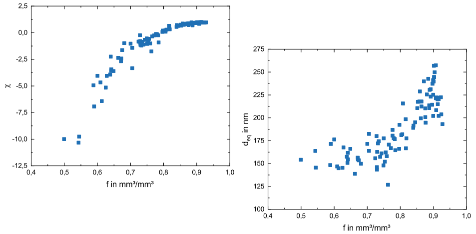

Impact of Pore Structure Properties

$$\frac{\bar{\sigma}}{\sigma} = \frac{\bar{\sigma}}{\sigma}(d_{eq}, SF, N, \chi, f, S_m)$$

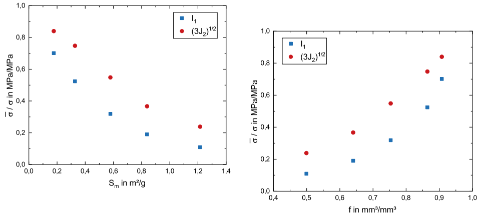

Homogenization and Modeling

Structure Homogenization

$$\zeta = \zeta(d_{eq}, SF, N, \chi, f, S_m)$$

Impact Functions

$$\theta, \vartheta = \theta(\zeta), \vartheta(\zeta)$$

Continuity Tensor

$$\mathbb{M} = \mathbb{M}(\theta, \vartheta)$$

Materials Modeling for Sintered Silver

Scale Transition Modeling

A. J. Carr, X. Milhet, P. Gadaud, S. A.E. Boyer, G. E. Thompson, and P. Lee. Quantitative characterization of porosity and determination of elastic modulus for sintered micro-silver joints. Journal of Materials Processing Technology, 225:19–23, 2015. ISSN 09240136. doi: 10.1016/j.jmatprotec.2015.03.037.
B. A. A. Wereszczak, D. J. Vuono, H. Wang, M. K. Ferber, and Z. Liang. Properties of bulk sintered silver as a function of porosity, 2012.
C. S. Zabihzadeh, S. van Petegem, M. Holler, A. Diaz, L. I. Duarte, and H. van Swygenhoven. Deformation behavior of nanoporous polycrystalline silver. part i: Microstructure and mechanical properties. Acta Materialia, 131:467–474, 2017. ISSN 13596454. doi: 10.1016/j.actamat.2017.04.021.

- Continuum isotropic linear elasticity as defined by "Hooke"

$$\boldsymbol{\sigma} = \mathbb{C} : \boldsymbol{\varepsilon}^{el} \qquad \text{and} \qquad \mathbb{C} = K\,\boldsymbol{I} \otimes \boldsymbol{I} + 2G\left(\mathbb{I} - \frac{1}{3}\boldsymbol{I} \otimes \boldsymbol{I}\right)$$

- Application of the new scale transition model yields

$$\overline{\boldsymbol{\sigma}} = \mathbb{M} : \mathbb{C} : \overline{\boldsymbol{\varepsilon}}^{el}$$

- Calculation of an effective Young's modulus to compare model prediction with experimental results from literature

$$\bar{E} = \frac{9G\theta K\vartheta}{3K\vartheta + G\theta}$$

- Good compromise between published experimental results

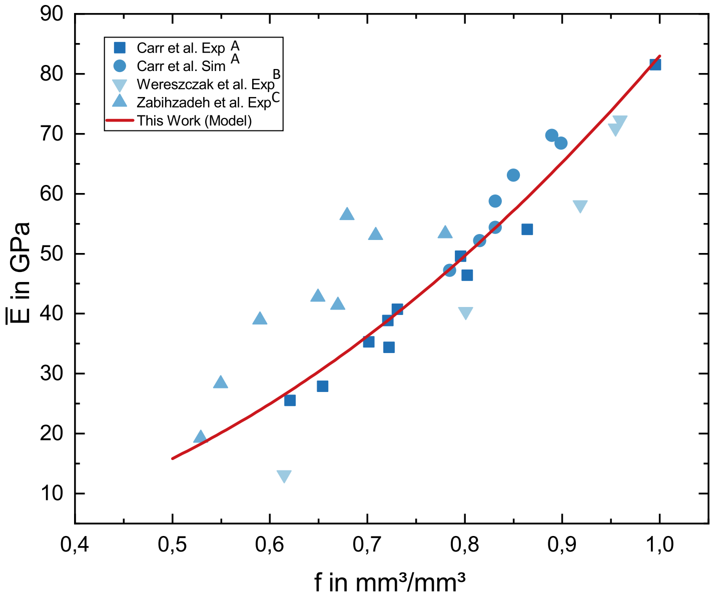

Effective elastic modulus for sintered silver as function of the fractional density f.

Materials Modeling for Sintered Silver

A Plastic Yield Locus Model

- Plastic yield locus describes surface in normal stress space
  - Elastic deformation: $\Phi < 0$
  - Plastic deformation: $\Phi = 0$
- Formulation of a new macroscopic yield surface function
- Impact of shear and hydrostatic loads considered
- Impact of sintering structure considered
- At $f = 1$, the von Mises yield function is obtained

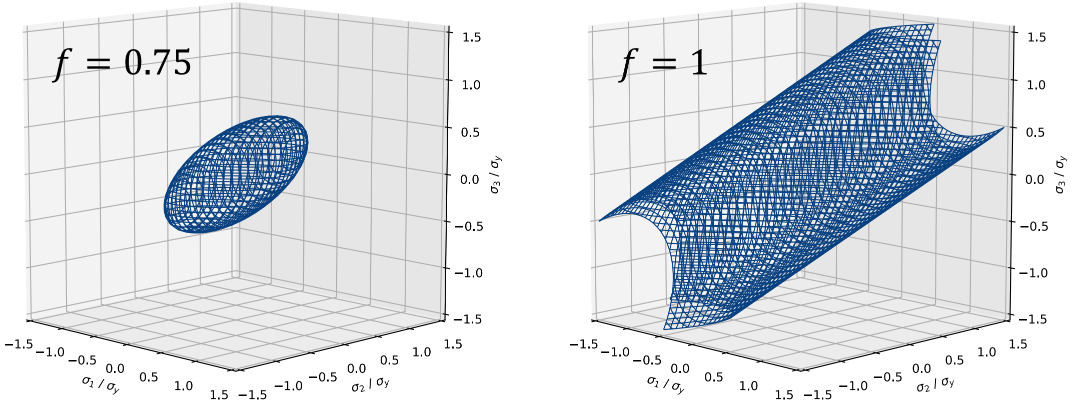

Yield surface fo sintered silver at different fractional densities f.

General Stress State: $\bar{\boldsymbol{\sigma}} = \begin{bmatrix} \bar{\sigma}_{11} & \bar{\sigma}_{12} & \bar{\sigma}_{13} \\ \bar{\sigma}_{21} & \bar{\sigma}_{22} & \bar{\sigma}_{23} \\ \bar{\sigma}_{31} & \bar{\sigma}_{32} & \bar{\sigma}_{33} \end{bmatrix}$ ⇨ 2nd-Order Tensor

Yield function: $\Phi = \bar{\sigma}_{eq}^2 + \omega(\zeta)\bar{\sigma}_h^2 - R - \sigma_y^2$ ⇨ Scalar-Valued

Deviator Impact

Dilatation Impact

Strain Hardening

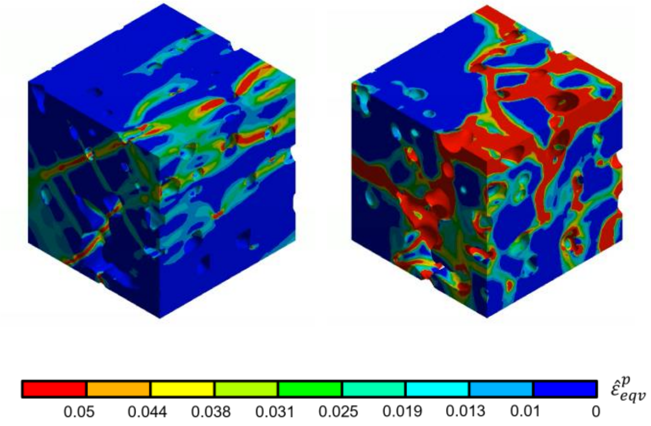

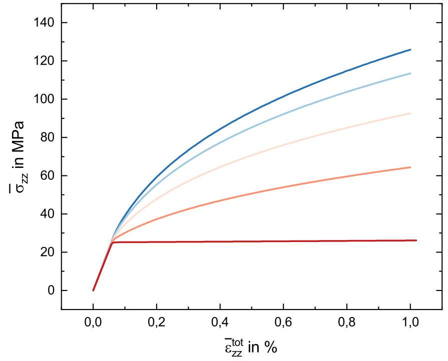

Tensile Stress-Strain Curves

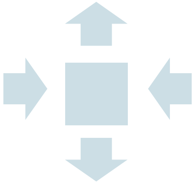

Shear Loading

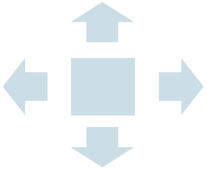

Hydrostatic Loading

Uniaxial Tensile Loading

Materials Modeling for Sintered Silver

A Plastic Yield Locus Model

- Comparison with Gurson-Tvergaard-Needleman model (GTN)

$$F = \left(\frac{\sigma_{eq}}{\sigma_y}\right)^2 + 2q_1(1-f)cosh\left(\frac{3}{2}q_2\frac{\sigma_h}{\sigma_y}\right) - (1+q_3(1-f)^2)$$

- Comparison with the results from the RVE simulations
- Comparison with tensile experiments from the literature
- Overall prediction is 43% better than a fitted GTN model

Orthogonal mean distance in MPa between yield surface model and FEM RVE simulation (assumed $\sigma_y = 100$ MPa for matrix material).

Model ↓ / f →	0.91	0.86	0.75	0.64	0.50	Sum
Qiu & Weng[C]	27.9	25.6	23.3	27.8	23.0	127.6
GTN (Fritzen et al.)[B]	13.0	14.5	13.7	18.2	18.9	78.3
GTN (Original)[A]	10.6	12.4	9.5	9.1	2.2	43.8
GTN (Fitted)	2.2	3.7	2.3	4.1	6.4	18.7
This Work	4.4	2.7	1.7	0.5	1.4	**10.7**

A. Needleman, V. Tvergaard, and J. W. Hutchinson. Void growth in plastic solids. Topics in Fracture and Fatigue, 56:145–178, 1992. doi: 10.1007/978-1-4612-2934-6{\textunderscore}4.
B. Fritzen, S. Forest, T. Böhlke, D. Kondo, and T. Kanit. Computational homogenization of elasto-plastic porous metals. International Journal of Plasticity, 29(2): 102–119, 2012. ISSN 07496419. doi: 10.1016/j.ijplas.2011.08.005.
C. Y. P. Qiu and G. J. Weng. A theory of plasticity for porous materials and particlereinforced composites. Journal of Applied Mechanics, 59(2):261–268, 1992. ISSN0021-8936. doi: 10.1115/1.2899515.

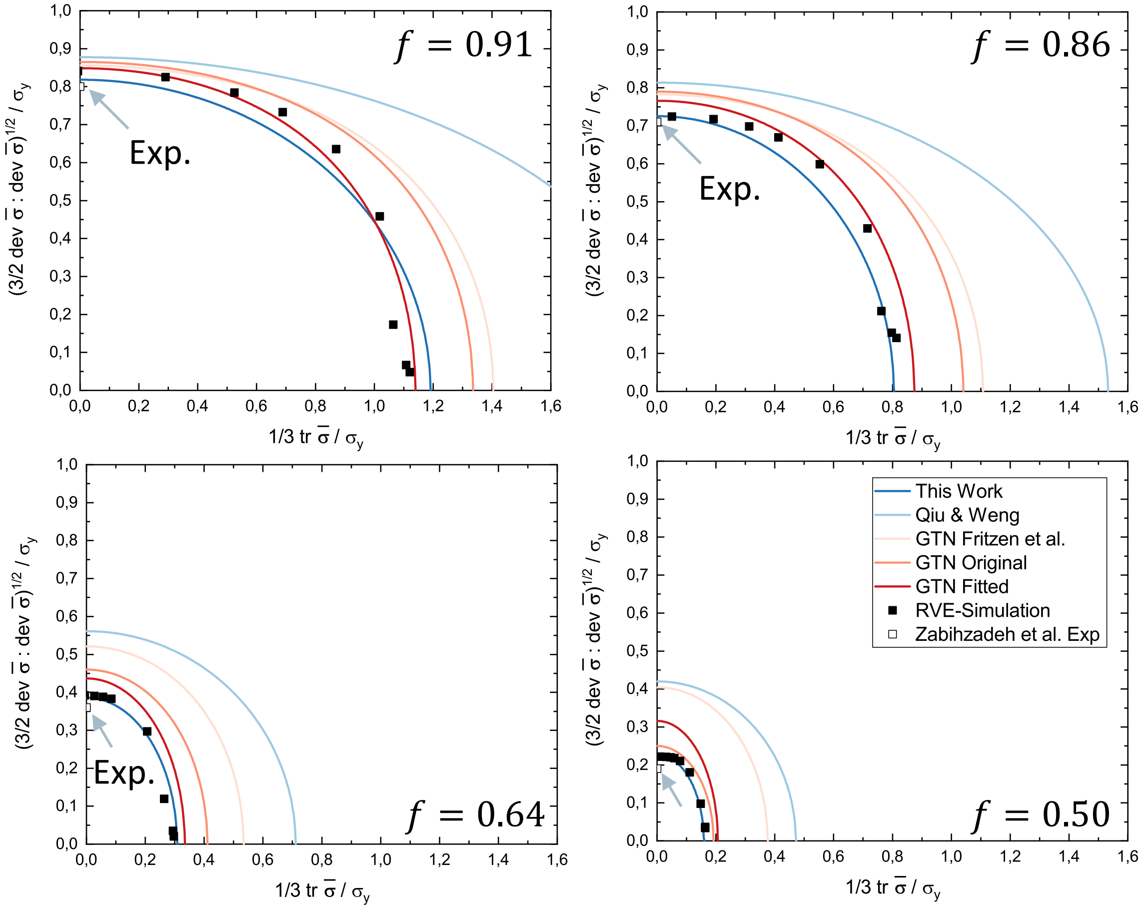

Adhesion Strength of Metallic Thin Films

Problem Description

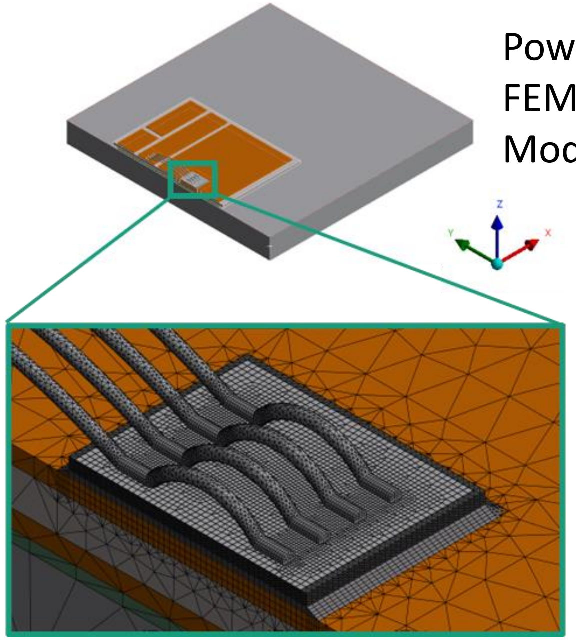

Power Cycling FEM Simulation Model (half)

- Power cycling FEM simulation shows maximum of equivalent stress and plastic strain (absolute and range / cycle) at the transition between chip and solder layer (corner and edge regions)
- Failure is likely to initiate there (if no further large defects are present)
- A long-living and reliable chip assembly requires a robust <u>joining material</u> and <u>chip back-end metallization</u> system

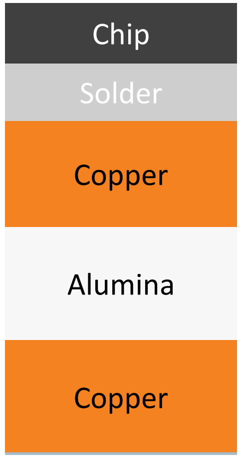

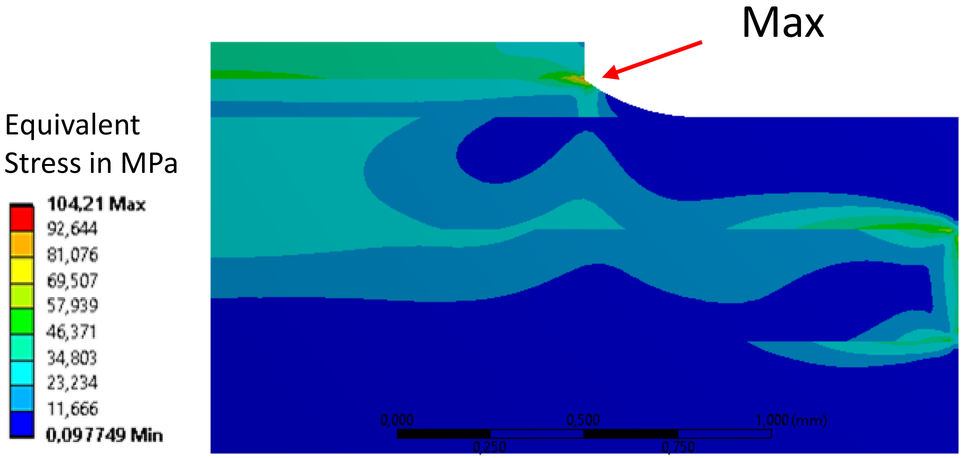

Max

Equivalent Stress in MPa

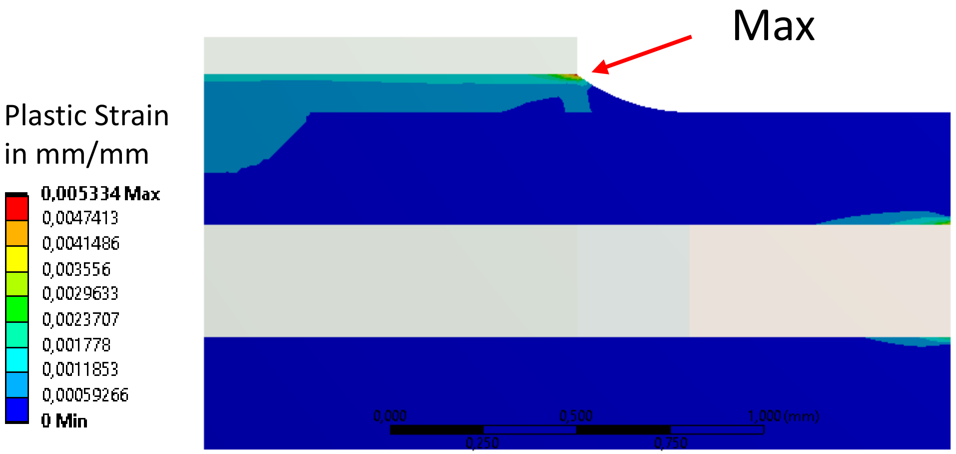

Max

Plastic Strain in mm/mm

Adhesion Strength of Metallic Thin Films
Problem Description

- Problem: Increased stress by change from Si to SiC devices
- Delamination of chip back-end metallization
  - During manufacturing: dicing, pick-up, etc.
  - During testing: thermal shock tests

- Evaluation of thin film adhesion by
  - Scotch tape tests
  - Cross-cut tests
  - Bending tests
  - Bulge tests
  - …
  - **Cross-Sectional-Nanoindentation (CSN)**

- Following slides are based on:

  Zhao, D., Letz, S.A., Jank, M., & März, M. (2024). Hierarchical Inverse Analysis of Adhesion Strength of Metal Thin Films on Semiconductor Substrate Via Cross-Sectional Nanoindentation. (Unpublished, In review).

Delamination of back-end metallization during wafer dicing.

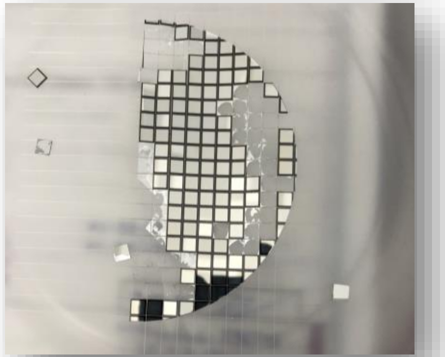

Delamination of back-end metallization during chip pick-up.

U. Waltrich, "Optimierung von Hochspannungsleistungsmodulen für modulare Multilevel-Topologien unter Berücksichtigung von Lebensdaueraspekten," Doctoral Thesis, Friedrich-Alexander-Universität Erlangen-Nürnberg (FAU), 2019.

Adhesion Strength of Metallic Thin Films

Cross-Sectional-Nanoindentation

- Steps in Cross-Sectional-Nanoindentation (CSN)
  - Preparation of smooth cross-section
  - Nanoindentation on substrate close to thin film interface
  - Si-wedge separates from the substrate
  - Lateral motion of Si-wedge delaminates thin film
  - Plateau in Load-Depth curve marks delamination stage
  - Remaining crack geometry can be studied in Front-View

- Evaluation of thin film adhesion by
  - S-Index (crack geometry, no physical property)
  - Adhesion strength (analytically accesible only by strong simplifications (geometry, linear material behavior, …))

Schematic Illustration of CSN

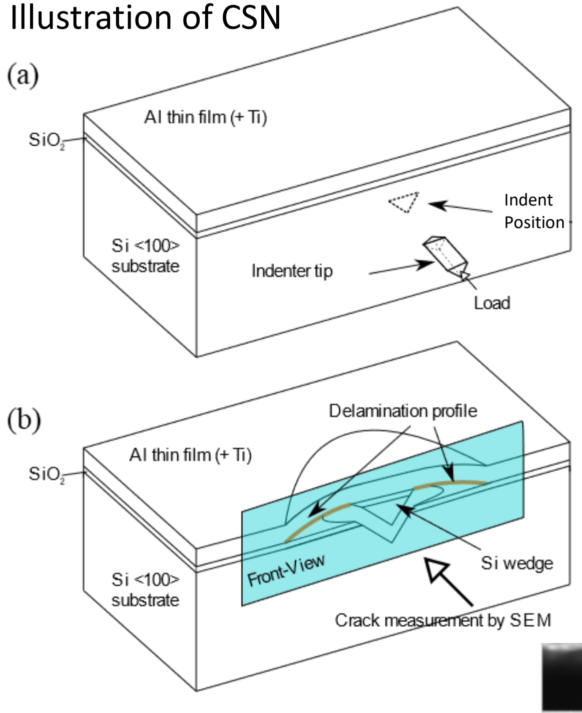

Load-Depth Curves during CSN

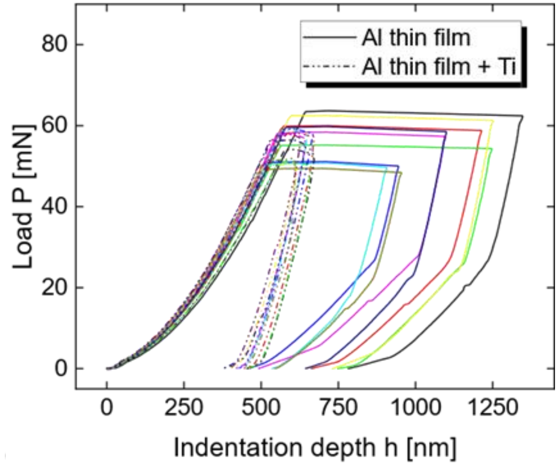

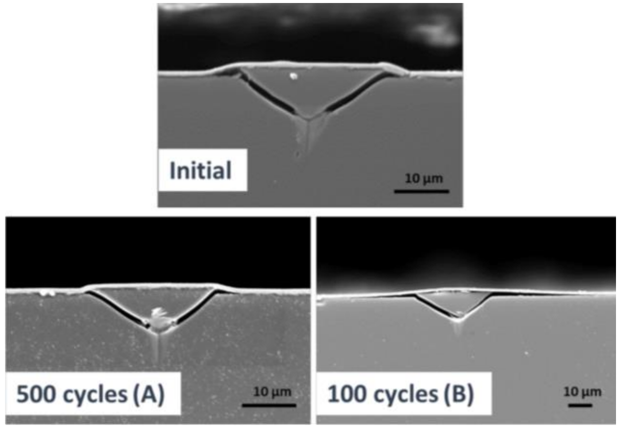

SEM Images in Front-View after CSN

Adhesion Strength of Metallic Thin Films

CSN Analysis by FEM Modeling

- 3D FEM simulation of CSN with Cohesive-Zone-Model (CZM) and parameter optimization based on experimental results
- Substrate fracture neglected; only thin film delamination simulated
- Requires knowledge of Si-wedge geometry and thin film properties
- Optimization objective: crack geometry in Front-View
- Parameters: critical strain energy release rate $G_{c,I}$ and the maximum normal cohesive traction σ_{max}

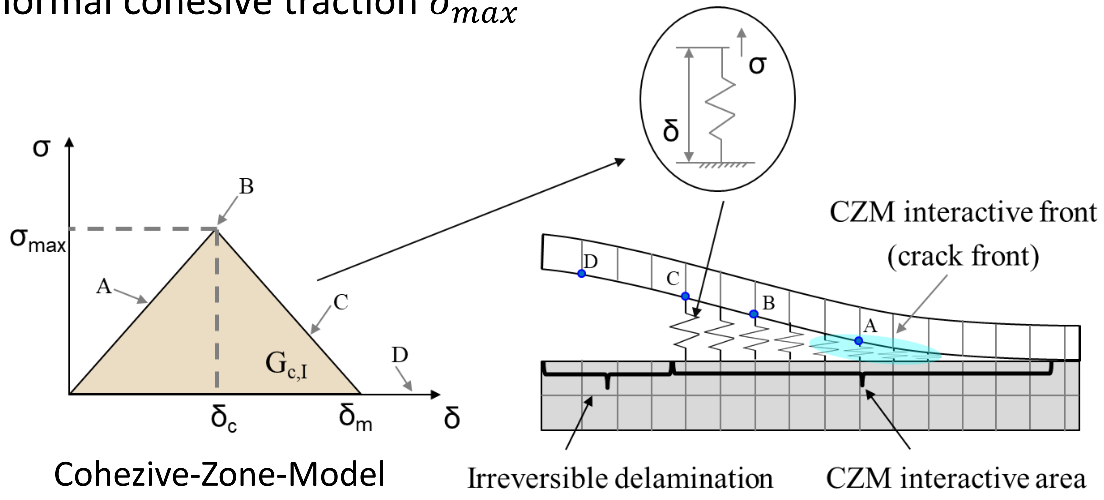

Cohezive-Zone-Model

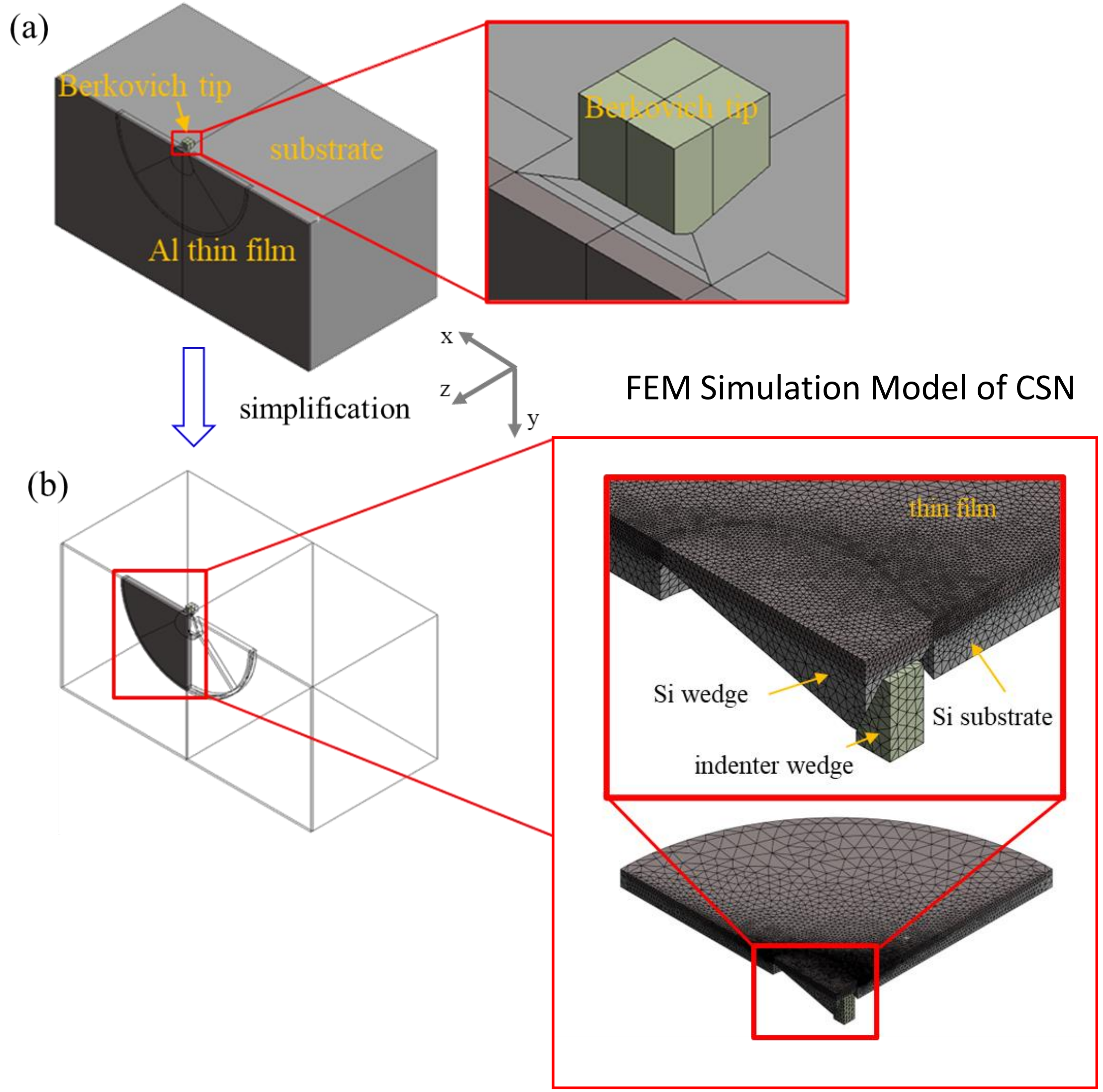

FEM Simulation Model of CSN

Adhesion Strength of Metallic Thin Films

CSN Analysis by FEM Modeling

- Simplex minimization of L^2-norm error between experimental and simulated interface crack profile

- Study of effect of Ti interim layer in Al/SiO2/Si system
  - **Al/SiO2/Si**: error = 2.3 nm (10 % SEM resolution)
    $G_{I,c} = 0.508\ J/m^2$ and $\sigma_{I,max} = 71.5\ MPa$
  - **Al/Ti/SiO2/Si**: error = 0.7 nm (5 % SEM resolution)
    $G_{I,c} = 22.3\ J/m^2$ and $\sigma_{I,max} = 80.4\ MPa$

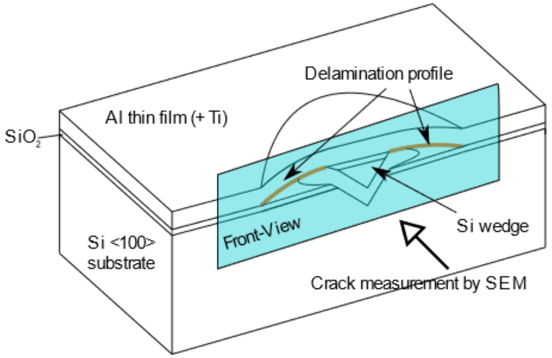

Delamination Profile

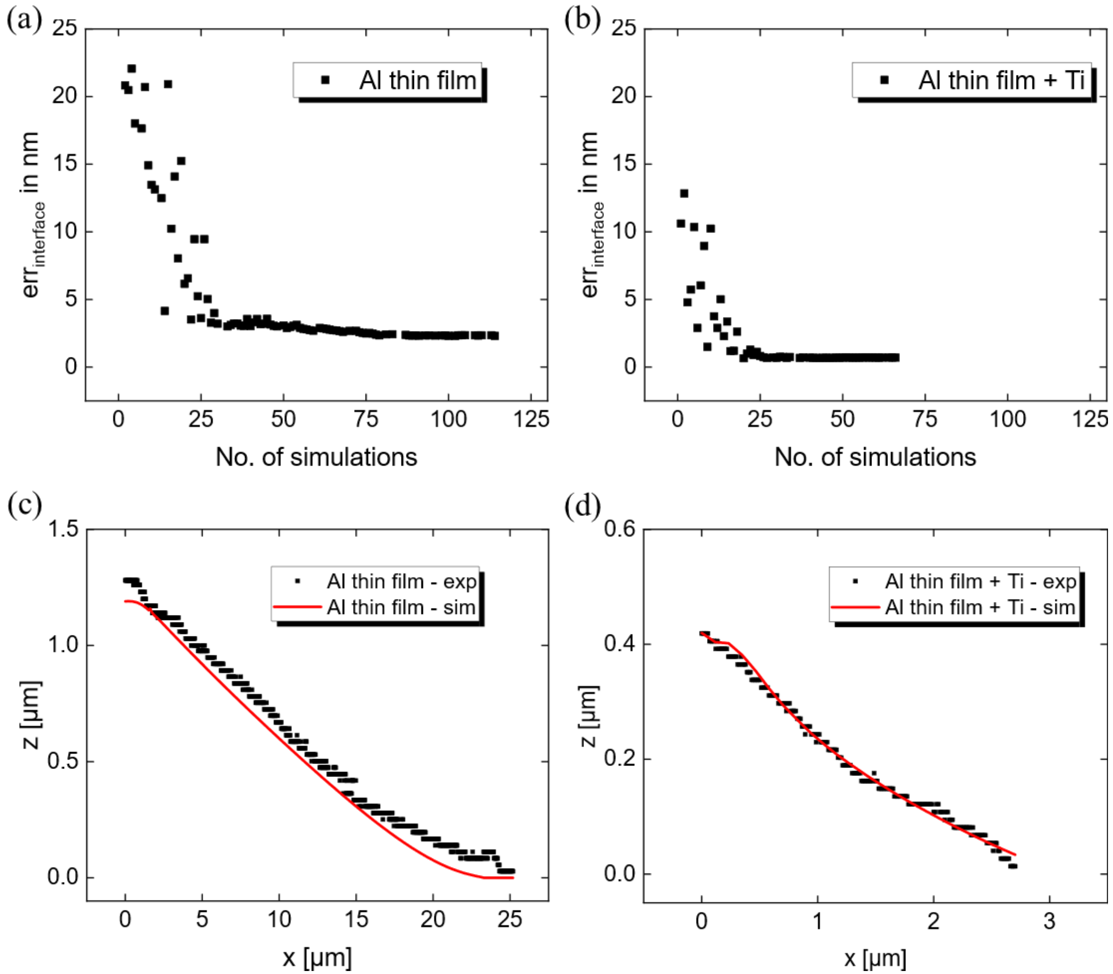

Adhesion Strength of Metallic Thin Films

CSN Analysis by FEM Modeling

- Benefits of proposed simulation approach
  - Quantitative assessment of adhesion strength
  - Insights into stress state enables comparability
  - Considers plastic dissipation of thin film
  - Higher level of physical details increases accuracy

Approach	$G_{I,c}{}^{Al}$ in J/m²	$G_{I,c}{}^{AlTi}$ in J/m²	$G_{I,c}{}^{AlTi}/G_{I,c}{}^{Al}$	**Remark**
A	4.35	924	212	*Analytic solution*: end-state; half-circular wedge geometry; without plasticity
B, C	0.23	8.24	36.8	*2D FE-model*: end-state; total internal energy used as debonding energy
this work	0.51	22.3	43,7	*3D FE-model with CZM*: real wedge geometry, delamination and backspring

A. J.M. Sánchez, S. El-Mansy, B. Sun, T. Scherban, N. Fang, D. Pantuso, W. Ford, M.R. Elizalde, J.M. Martínez-Esnaola, A. Martín-Meizoso, J. Gil-Sevillano, M. Fuentes, J. Maiz, Cross-sectional nanoindentation: a new technique for thin film interfacial adhesion characterization, Acta Materialia 47 (1999) 4405–4413. https://doi.org/10.1016/S1359-6454(99)00254-2.

B. M.R. Elizalde, J.M. Sánchez, J.M. Martínez-Esnaola, D. Pantuso, T. Scherban, B. Sun, G. Xu, Interfacial fracture induced by cross-sectional nanoindentation in metal–ceramic thin film structures, Acta Materialia 51 (2003) 4295–4305. https://doi.org/10.1016/S1359-6454(03)00256-8.

C. S. Roy, E. Darque-Ceretti, E. Felder, H. Monchoix, Cross-sectional nanoindentation for copper adhesion characterization in blanket and patterned interconnect structures: experiments and three-dimensional FEM modeling, Int J Fract 144 (2007) 21–33. https://doi.org/10.1007/s10704-007-9072-7.

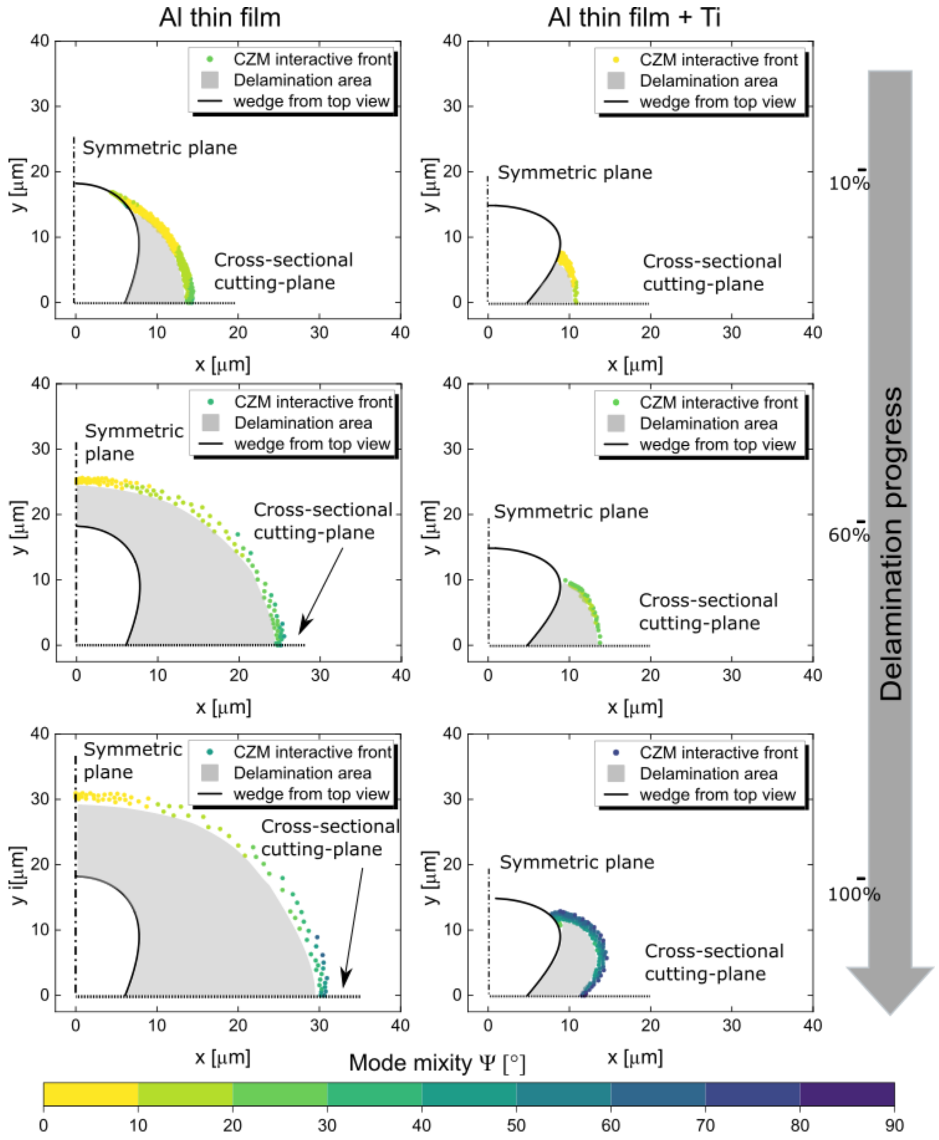

Conclusions

- There is a broad range of tasks in the reliability and test environment, which can/must be solved by FEM simulations

- Inelastic material models and their calibration are essential for accurate simulation results
  - Sintered silver interconnects are non-continuous at the mesoscale
  - Porosity impact can be studied by FEM simulations with RVEs → “digital material characterization”
  - Results allow for formulating macroscopic behavior laws, which can be implemented in FEM code

- The back-end metallization plays a crucial role in the process yield / device reliability
  - Cross-Sectional-Nanoindentation can be used to study the adhesion behavior of thin films
  - Its inverse FEM simulation along with parameter optimization enables access to physical interface properties and deeper insights into stress state and roles of adhesion-contributing mechanisms (ductility)

- Outlook: Many tasks in our field require to model mechanisms, which occur simultaneously on multiple length/time scales
  - Surface roughness, grain size and orientation, texture, residual stresses, … → thin film adhesion
  - Local crack nucleation and macroscopic growth over millions of thermal cycles (nonlinear process)

Fraunhofer Institute for Integrated
Systems and Device Technology IISB

Contact

Sebastian A. Letz
Vehicle Electronics / Test & Reliability
Tel. +49 9131 761 619
sebastian.letz@iisb.fraunhofer.de